SUPPORTING INFORMATION

Supramolecular-Surface Photochemistry: Cascade Energy Transfer between Encapsulated Dyes Aligned on Clay Nano-sheet Surface

Takamasa Tsukamoto [a, b], Elamparuthi Ramasamy [c], Tetsuya Shimada [d], Shinsuke Takagi* [d] and V. Ramamurthy* [c]

[a] Department of Chemistry, Graduate School of Science, The University of Tokyo, 7-3-1, Hongo, Bunkyo-ku, Tokyo 113-0033, Japan

[b] Japan Society for the Promotion of Science (JSPS / PD), Ichibancho, Chiyoda-ku, Tokyo 102-8471, Japan

[c] Department of Chemistry, University of Miami, Coral Gables, Florida 33146-0431, United States of America

[d] Department of Applied Chemistry, Graduate Course of Urban Environmental Sciences, Tokyo Metropolitan University, 1-1, Minami-ohsawa, Hachiohji-shi, Tokyo 192-0397, Japan

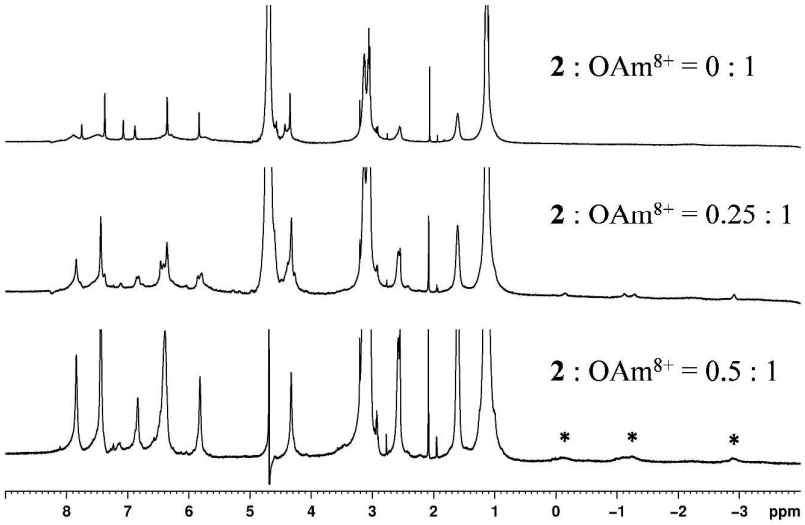

Figure S1. ^{1}H-NMR spectra for 0.5 mM **2** and 1 mM OAm^{8+} (**1**) at 0.5 : 1 in 0.1M DCl / D_2O (pH = 2.1). The guest peaks were marked with asterisk (*).

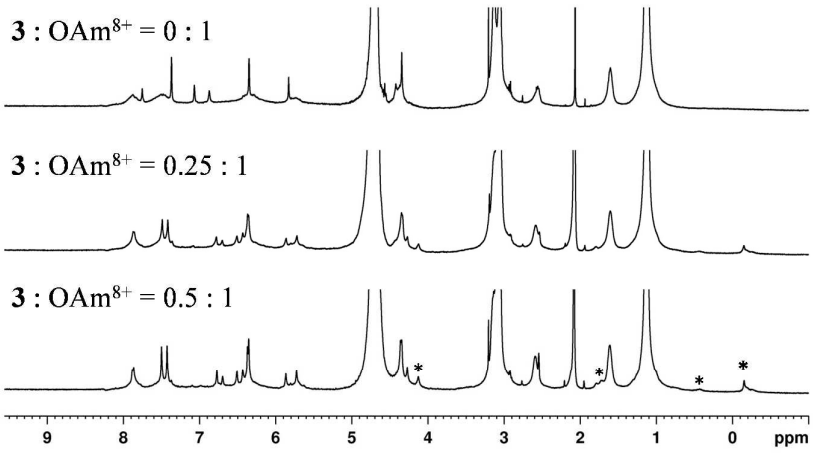

Figure S2. ^{1}H-NMR spectra for 0.5 mM **3** and 1 mM OAm^{8+} (**1**) at 0.5 : 1 in 0.1M DCl / D_2O (pH = 2.1). The guest peaks were marked with asterisk (*).

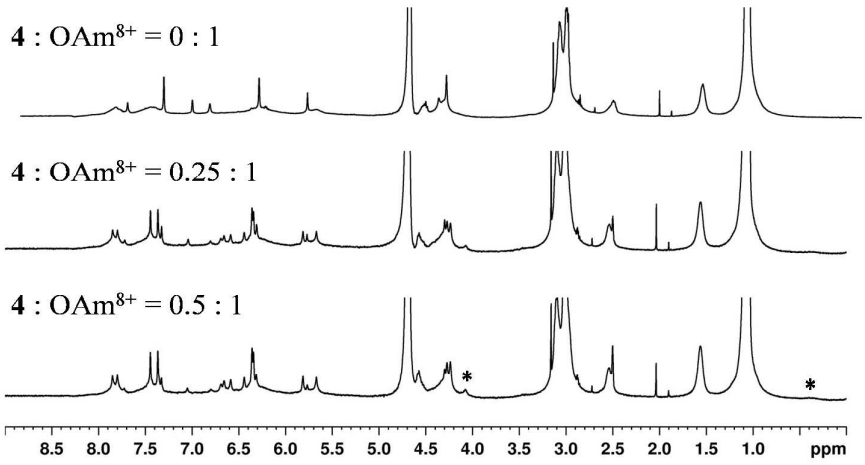

Figure S3. ^{1}H-NMR spectra for 0.5 mM **4** and 1 mM OAm^{8+} (**1**) at 0.5 : 1 in 0.1M DCl / D_2O (pH = 2.1). The guest peaks were marked with asterisk (*).

In Figure S1-S3, The ^{1}H NMR signals of OAm in D_2O/DCl at 1 mM are broad due to aggregation. But, the signals are getting sharper and well separated after gradual addition of guests **2**, **3** and **4**. For guest **3** and **4**, the splitted host peaks from 5 to 8 ppm (aromatic region) tell that they are experiencing different guest (unsymmetrical). Moreover, for all guests, it is clearly seen the encapsulated guest proton signals are in the upfield region of ^{1}H NMR spectra (Fig S1 and S2). This concludes that the encapsulation of guests within OAm.

And these NMR spectral behaviors of **2**, **3** and **4** capsulated in OAm and those forming (2:1) (OA:guest) complexes (OA is an anionic cavitand having similar molecular structure to OAm) in literature[1,2] are in conforming well. This suggests that these guest molecules are within the OAm and form (2:1) (OAm:guest) complexes.

Additionally, the emission spectra of **3**, **4** in water showed at 490 nm and 547 nm respectively, but when these guests molecules within OA, the emission λ_{max} moved to 424 and 480

nm respectively[1]. Similarly, the guest molecules **3** and **4** in OAm solution in this paper show the emission λ_{max} at 420 and 480 nm. This evidence strongly suggests that these guest molecules formed (2:1) complexes with OAm. On the other hand, the guest molecule **2** in OAm solution almost did not show any emission spectral shifts. This result is also reasonable because the emission maxima (λ_{max} at 395 nm) of **2** did not change by capsulation with OA in literature.[2]

[1] Gupta, S.; Adhikari, A.; Mandal, A. K.; Bhattacharyya, K.; Ramamurthy, V. Ultrafast Singlet-Singlet Energy Transfer between an Acceptor Electrostatically Attached to the Walls of an Organic Capsule and the Enclosed Donor. *J. Phys. Chem. C* **2011**, *115*, 9593–9600.

[2] Porel, M.; Jayaraj, N.; Kaanumalle, L. S.; Maddipatla, M. V. S. N.; Parthasarathy, A.; Ramamurthy, V. Cavitand Octa Acid Forms a Nonpolar Capsuleplex Dependent on the Molecular Size and Hydrophobicity of the Guest. *Langmuir* **2009**, *25*, 3473-3481.

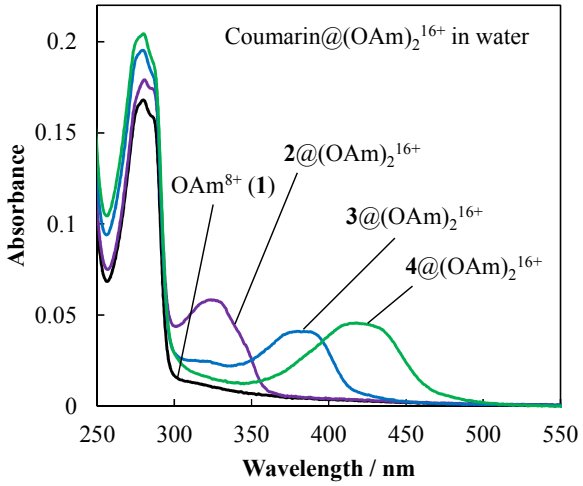

Figure S4. Absorption spectra for 10 μM free OAm^{8+} (**1**), 5.0 μM **2**@$(OAm)_2^{16+}$, 5.0 μM **3**@$(OAm)_2^{16+}$ and 5.0 μM **4**@$(OAm)_2^{16+}$ in 0.1M HCl aqueous solution.

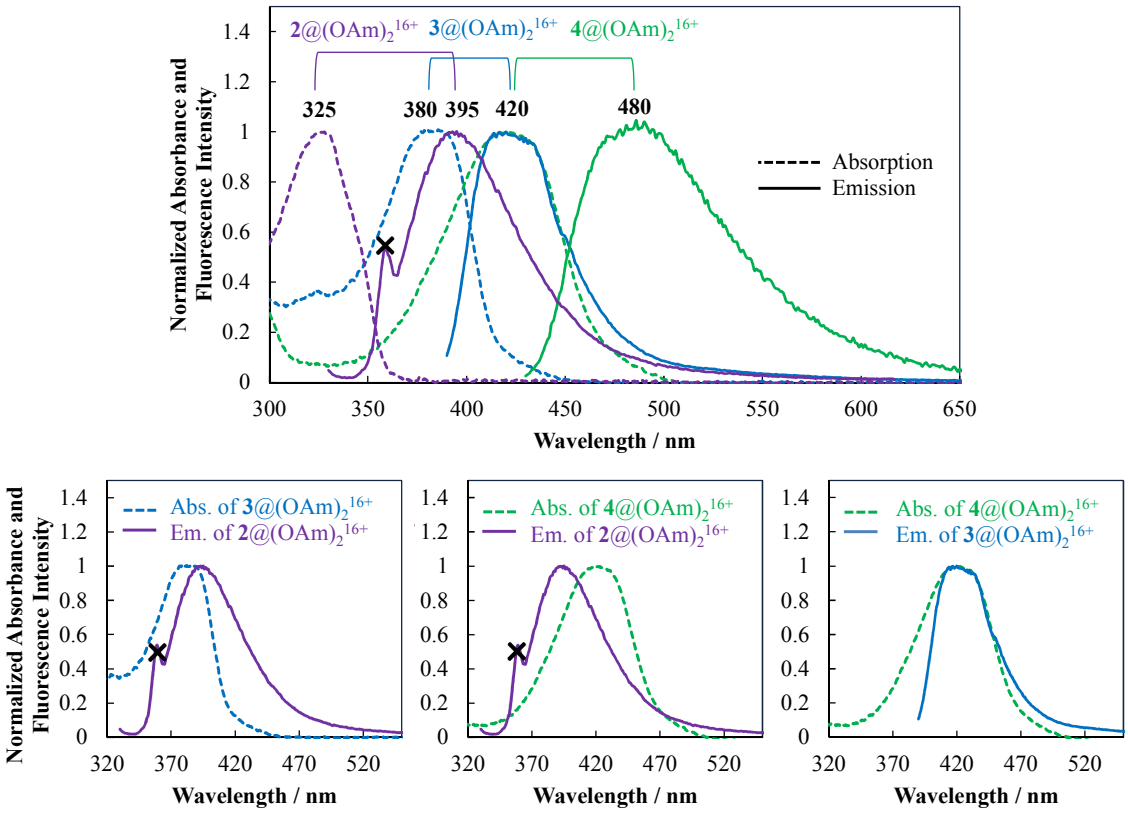

Figure S5. Normalized absorption spectra for 5.0 μM **2**@$(OAm)_2^{16+}$, **3**@$(OAm)_2^{16+}$ and **4**@$(OAm)_2^{16+}$ in 0.10 M HCl aqueous solution (The absorption spectra of 10 μM free OAm^{8+} (**1**) were deducted from those of coumarin@$(OAm)_2^{16+}$) and normalized fluorescence spectra for 0.50 μM **2**@$(OAm)_2^{16+}$, **3**@$(OAm)_2^{16+}$ and **4**@$(OAm)_2^{16+}$ in 1.0 M HCl aqueous solution.

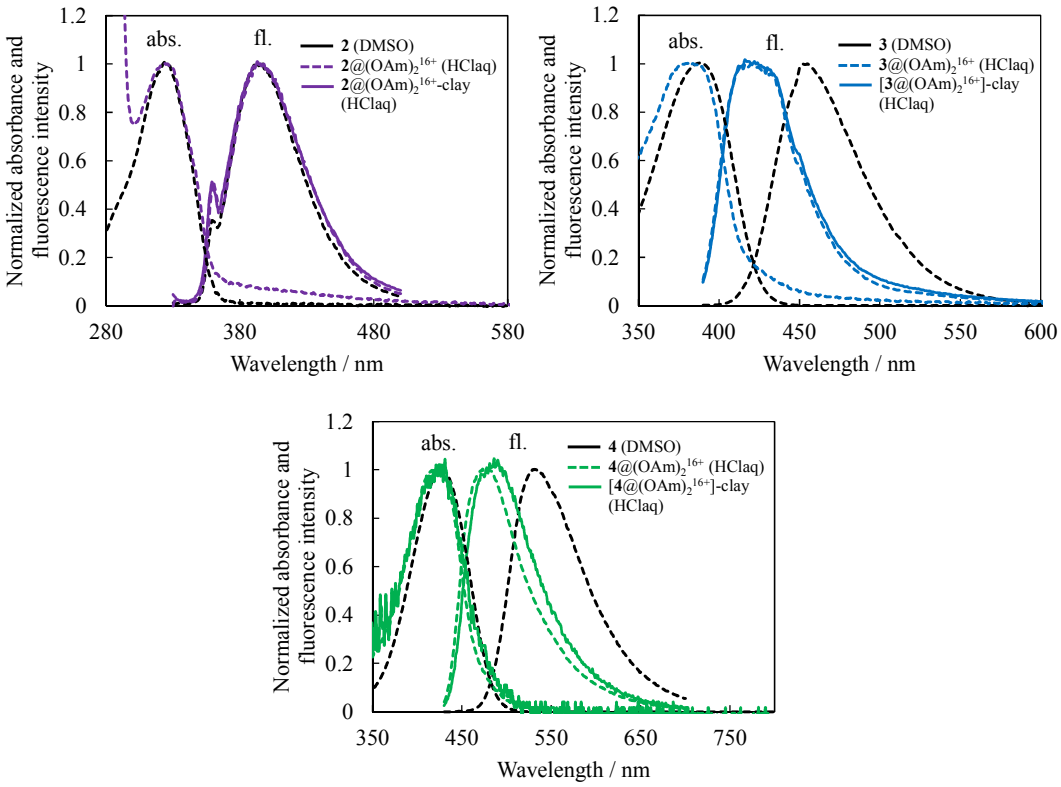

Figure S6. Normalized absorption and emission spectra for free coumarin in DMSO, coumarin@$(OAm)_2^{16+}$ and [coumarin@$(OAm)_2^{16+}$]-clay in 1.0 and 0.10 M HCl aqueous solution for absorption and emission.

In Figure S6, the absorption spectra of capsulated coumarins with clay were observed only for [**4**@$(OAm)_2^{16+}$]-clay because the absorption spectra cannot be measured in shorter wavelength region than absorption of [**4**@$(OAm)_2^{16+}$]-clay due to limit of resolution. And [coumarin@$(OAm)_2^{16+}$]-clay showed sedimentation behavior at concentration for absorption measurement and its absorbance decreased. So it was difficult to measure their absorption spectra with high intensity. However, there are no influences for investigation of energy transfer because this sedimentation behavior was completely not suppressed at lower concentration for fluorescence measurement.

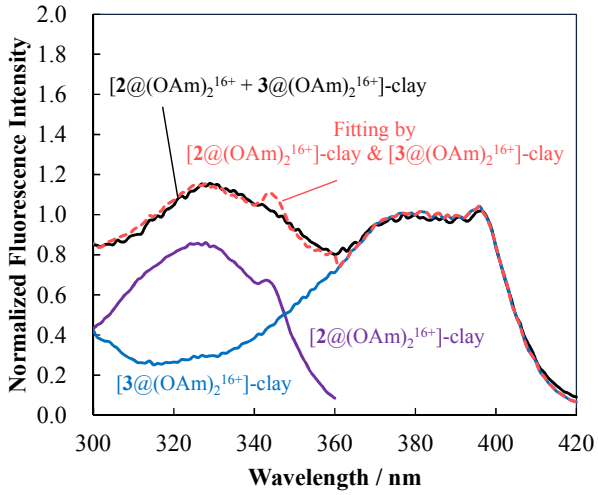

Figure S7. Normalized excitation spectra for [**2**@$(OAm)_2^{16+}$ + **3**@$(OAm)_2^{16+}$]-clay, [**2**@$(OAm)_2^{16+}$]-clay, [**3**@$(OAm)_2^{16+}$]-clay complexes and fitting spectra. (The emission wavelength was 460 nm. The loading levels were set at 300% versus the CEC of the clay for all samples. [**2**@$(OAm)_2^{16+}$] = [**3**@$(OAm)_2^{16+}$] = 0.5 μM. [clay] = 5.3 μequiv. L^{-1}.)

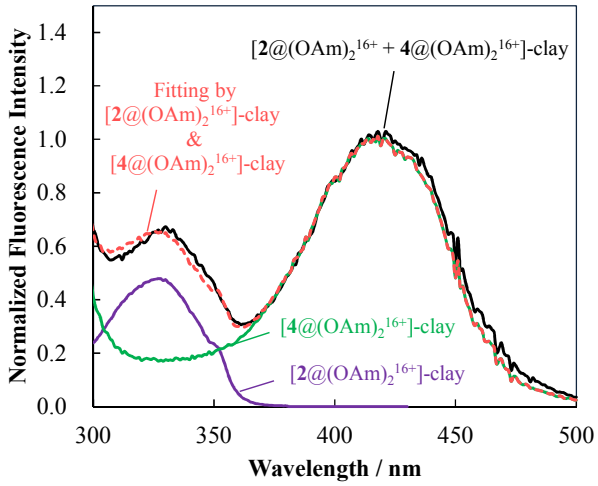

Figure S8. Normalized excitation spectra for [**2**@$(OAm)_2^{16+}$ + **4**@$(OAm)_2^{16+}$]-clay, [**2**@$(OAm)_2^{16+}$]-clay, [**4**@$(OAm)_2^{16+}$]-clay complexes and fitting spectra. (The emission wavelength was 550 nm.

The loading levels were set at 300% versus the CEC of the clay for all samples. [**2**@$(OAm)_2^{16+}$] = [**4**@$(OAm)_2^{16+}$] = 0.5 μM. [clay] = 5.3 μequiv. L^{-1}.)

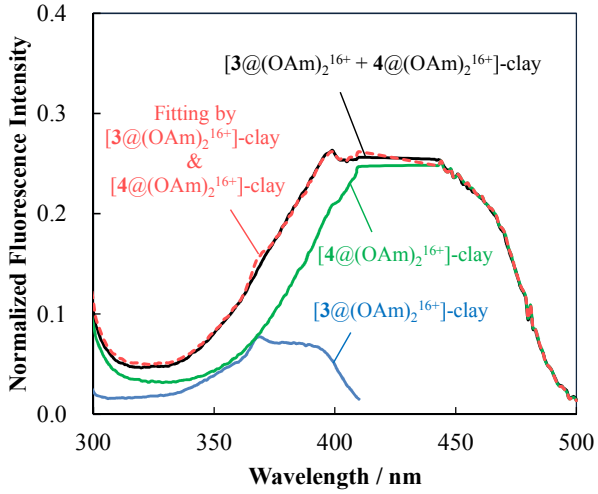

Figure S9. Normalized excitation spectra for [**3**@$(OAm)_2^{16+}$ + **4**@$(OAm)_2^{16+}$]-clay, [**3**@$(OAm)_2^{16+}$]-clay, [**4**@$(OAm)_2^{16+}$]-clay complexes and fitting spectra. (The emission wavelength was 480 nm. The loading levels were set at 300% versus the CEC of the clay for all samples. [**3**@$(OAm)_2^{16+}$] = [**4**@$(OAm)_2^{16+}$] = 0.5 μM. [clay] = 5.3 μequiv. L^{-1}.)

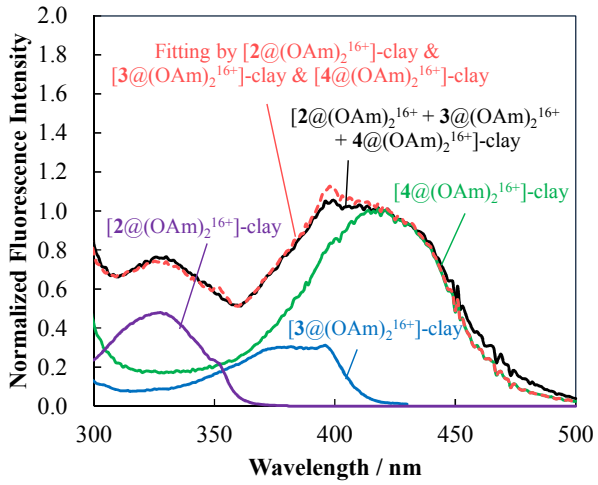

Figure S10 Normalized excitation spectra for [**2**@$(OAm)_2^{16+}$ + **3**@$(OAm)_2^{16+}$ + **4**@$(OAm)_2^{16+}$]-clay, [**2**@$(OAm)_2^{16+}$]-clay, [**3**@$(OAm)_2^{16+}$]-clay, [**4**@$(OAm)_2^{16+}$]-clay complexes and fitting spectra. (The

emission wavelength was 550 nm. The loading levels were set at 300% versus the CEC of the clay for all samples. [**2**@$(OAm)_2^{16+}$] = [**3**@$(OAm)_2^{16+}$] = [**4**@$(OAm)_2^{16+}$] = 0.5 μM. [clay] = 8.0 μequiv. L^{-1}.)

Table S1. Parameters for Calculations of Energy Transfer Efficiency in Three-component Sample

λ_{ex} / nm	α	β	γ	I^A / 10^{-3}	I^B / 10^{-3}	I^C / 10^{-3}	$\eta_{ET}{}_B^A$	$\eta_{ET}{}_C^A$	$\eta_{ET}{}_C^B$	$\Phi_q{}^A$	$\Phi_q{}^B$	$\Phi_q{}^C$
320	0.35	0.73	6.0	4.5	1.2	0.41	32%	34%	33%	0%	33%	0%
380	-	0.33	1.6	-	3.6	2.0						

*λ_{ex} are excitation wavelengths. α, β and γ are coefficients of fluorescence intensity changes in **2**@$(OAm)_2^{16+}$, **3**@$(OAm)_2^{16+}$ and **4**@$(OAm)_2^{16+}$ to their spectra of individual sample. I^A, I^B and I^C are absorbance of them at excitation wavelengths. $\eta_{ET}{}^{AB}$, $\eta_{ET}{}^{AC}$ and $\eta_{ET}{}^{BC}$ is energy transfer efficiency. $\Phi_q{}^A$, $\Phi_q{}^B$ and $\Phi_q{}^C$ are energy loss efficiencies from them at excited states in the co-adsorption system.*

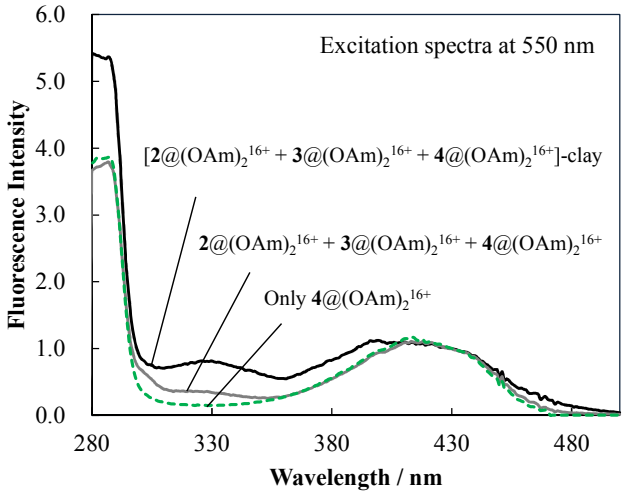

Figure S11. Normalized excitation spectra for [**2**@$(OAm)_2^{16+}$ + **3**@$(OAm)_2^{16+}$ + **4**@$(OAm)_2^{16+}$]-clay, only [**4**@$(OAm)_2^{16+}$]-clay complexes and mixture of [**2**@$(OAm)_2^{16+}$], [**3**@$(OAm)_2^{16+}$] and [**4**@$(OAm)_2^{16+}$] without clay. (The emission wavelength was 550 nm. The loading levels were set at

300% versus the CEC of the clay for all samples. [**2**@$(OAm)_2^{16+}$] = [**3**@$(OAm)_2^{16+}$] = [**4**@$(OAm)_2^{16+}$] = 0.5 μM.)